J. Biomed. Eng. Res : 310-317, 2006

A Mueller Matrix Study for Measuring Thermal Damage Levels of Collagenous Tissues

Jae-Hoon Jun

Department of Biomedical Engineering, College of Biomedical & Life Science, Konkuk University
Research Institute of Biomedical Engineering, Konkuk University
(Received October 9, 2006. December 1, 2006)

Abstract

Extensive research with polarimetry and Mueller matrix has been done for chemical measurements and possible cancer detection. However, the effect of thermally denatured biological tissue on polarization changes is not well known. The purpose of this study is to characterize polarization changes in collagen due to thermal denaturation. The variations in polarized state caused by thermal damage were investigated by obtaining the Mueller matrix elements of collagen sample at multiple thermal damage levels. The changes in birefringence of denatured collagen were also investigated. This information could be used to determine the extent of thermal damage level of clinically heat treated tissues.

Key words : thermally denatured tissue, collagen, mueller matrix, polarization

Ⅰ. INTRODUCTION

The non-invasive optical approaches utilizes the property of light such as intensity, orientation or polarization, and wavelength, after either being transmitted through or reflected from a tissue. Polarimetry, which can characterize the optically active materials such as glucose and biological tissues with the polarized light source, was first discovered in the early 1800s by Biot. Throughout the past decade, considerable research has been performed to utilize the concept of polarimetry for detecting the blood glucose levels in the body [1-5]. The principle of this technique is based on the ability of certain optically active molecules referred to as chiral molecules to rotate the incident polarized, or light propagating in a particular direction, through a certain angle. March and Rabinovitch proposed the eye as a suitable test site for the non-invasive detection of blood glucose using the Faraday effect [4,5]. They showed the glucose present in the aqueous humor of the eye could directly be correlated with the blood glucose levels.

Extensive research has been performed in developing a non-invasive polarimetric sensor which utilizes the anterior chamber of the eye as a potential test site [6-13]. Coté et al.[7] reported the potential for millidegree sensitivity with a system utilizing a true phase polarimetric techique. They developed an open-loop phase technique and theoretically accounted for the possible noise sources in the in vivo system. This work was followed by Goetz et al. [8], who built a system similar to that proposed by March, which was capable of microdegree accuracy. A multispectral system using a single pockel cell, that was capable of estimating the amount of glucose in the presence of other optically active molecules, was developed by King et al.[14]. Cameron et al. [13] took the development of a non-invasive polarimeter for glucose sensing a step forward by developing a digital closed-loop control for the optical system. This setup was similar to that of Goetz but improved considerably the repeatability and stability while maintaining the accuracy.

The concept of the Mueller matrix was developed by Hans Mueller in 1943. The Mueller matrix can mathematically characterize the polarization state of any optically active element. In conjunction, the Mueller-Stokes vector calculus can be utilized to determine mathematically the effect of an optical element on the change of incident light beam. To show the intimate relationship between the Stokes and the Mueller matrix, the complete polarization-scatter experiments were conducted by Bickel and Bailey [15] with highly motivated measurements. Bickel et al.[16] was the first to demonstrate that the useful information could be obtained by investigating the effect of polarization in scattered light of a biological material. Later, they showed the use of polarized light scattering as a tool for cell differentiation. The measurements were performed on biological cell suspensions and showed potential for cell characterization. Thus this research served as

Corresponding Author : Jae-Hoon Jun
Konkuk University, 322 Danwol-dong,
Chungju-si, Chungcheongbuk-do, South Korea 380-701
Tel : +82-43-840-3799 / FAX : +82-43-851-0620
E-mail : jjun81@kku.ac.kr

$$M=\begin{bmatrix} OO & HO-VO & PO-MO & RO-LO \\ OH-OV & (HH+VV)-(HV+VH) & (PH+MV)-(PV+MH) & (RH+LV)-(RH+LH) \\ OP-OM & (HP+VM)-(HM+VP) & (PP+MM)-(PM+MP) & (RP+LM)-(RM+LP) \\ OR-OL & (HR+LV)-(HL+VR) & (PR+MI)-(PL+MR) & (RR+LL)-(RL+LR) \end{bmatrix} \quad (3)$$

$$M=\begin{bmatrix} HH+HV+VH+VV & HH+HV-VH-VV & PH+PV-MH-MV & RH+RV-LH-LV \\ HH+VH-HV-VV & (HH+VV)-(HV+VH) & (PH+MV)-(PV+MB) & (RH+LV)-(RH+LH) \\ HP+VP-HM-VM & (HP+VM)-(HM+VP) & (PP+MM)-(PM+MP) & (RP+LM)-(RM+LP) \\ HR+VR-HL-VL & (HR+LV)-(HL+VR) & (PR+MI)-(PL+MR) & (RR+LL)-(RL+LR) \end{bmatrix} \quad (4)$$

the foundation for further research to characterize the polarization state of biological tissues and turbid media [17-21]. Zeitz et al. [22] reported the potential use of the differential scattering of circularly polarized light to probe polynucleosome superstructure. Furthermore, the spatially dependent intensity patterns of polarized light, that is diffusely back-scattered from turbid media, could be used to distinguish between normal and cancerous tissues [23]. Rakovic et al. [24] presented a numerical method for the simultaneous calculation of all 16 elements of the effective back-scattered Mueller matrix and also proved that there were only 7 independent elements in the 4x4 matrix.

The Monte Carlo technique was used in studying the backscattering of a polarized laser beam from a plane-parallel medium [25]. The degree of polarization of the diffuse light was investigated when the incident beam was right circularly polarized. Cameron et al. [26, 27] demonstrated a numerical method that allows the simultaneous calculation of 16 elements of the backscattering Mueller matrix. They used the Monte Carlo method to simulate the effective backscattered Mueller matrix for a polystyrene suspension.

II. METHODS

A. Mueller Matrix Theory and Data Acquisition

The Stokes vector S of a light beam is based on seven flux measurements with different analyzers in front of the detectors. In equation (1),

$$S=\begin{bmatrix} O \\ H-V \\ P-M \\ R-L \end{bmatrix} \quad (1)$$

O, H, V, P, M, R, and L are the intensities of unpolarized light, horizontally polarized light, vertically polarized light, + 45 degree polarized light, - 45 degree polarized light, right circularly polarized light, and left circularly polarized light.

The Mueller matrix of a sample transforms an incident Stokes vector into the corresponding output Stokes vector.

$$S_{out}=MS_{in} \quad (2)$$

In equation (2), S_{out}, $S_{\in}$, and M are output Stokes vector, incident Stokes vector, and Mueller matrix, respectively. The 4×4 Mueller matrix can be presented in equation 3. The symbols consisting of double polarization states represent detected signals with the input polarization state denoted by the left letter and the output polarization state denoted by the right letter. For example, HV refers to a detected signal with horizontally polarized input state (H) and vertically polarized output state (V).

Therefore, by exposing the sample to each polarization state, at each respective input state, the Mueller matrix of the sample can be reconstructed, in which a total of $7\times7=49$ separate images or detected signals must be required. The Mueller matrix can further be reduced by using the relation, $H+V=O$. Thus $6\times6=36$ detected signals need to be acquired to reconstruct the Mueller matrix of the sample.

The optical system for acquiring the Mueller matrix elements for the collagen sample is shown in Fig. 1. A laser diode (633 nm wavelength) was used to provide a input laser beam. The input laser beam was polarized via various polarization optics, such as the polarizer, polarization rotator, and variable retarder to obtain the desired input polarization. This beam after passing through input optics was directed onto the sample reflected by mirror and then imaged through polarization output (or analyzer) optics, which are similar to the input polarization optics, using the CCD camera (Lynxx 2000, Spectra Source Instruments, CA). The CCD camera was used at the final output stage to obtain the data under various combinations of input and output optics. The CCD array size was 338×244 and the pixel size was $10\times10\,\mu m^2$. The exposure time for the camera was set at 0.04 sec.

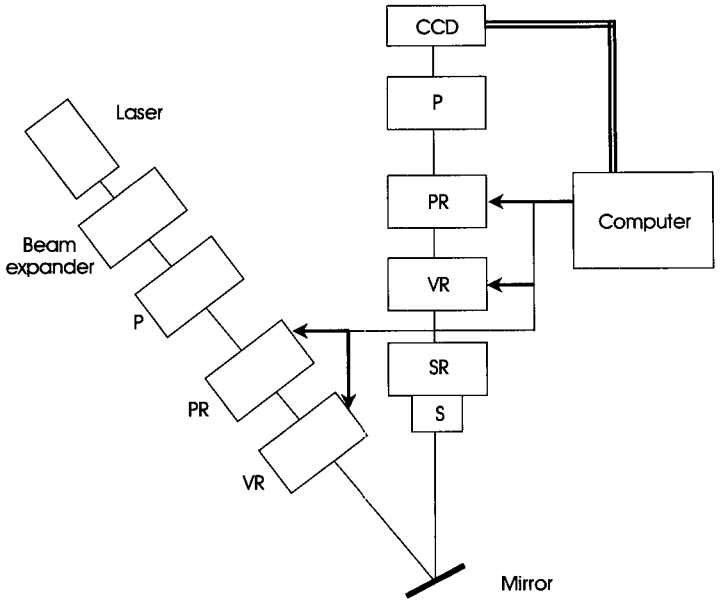

Fig. 1. The automated optical setup for obtaining the Mueller matrix of a sample.
(P: Polarizer, PR: Polarization Rotator, VR: Variable Retarder, S: Sample, SR: Sample Rotator)

The automated system includes polarizers, polarization rotators, and variable retarders to provide the necessary polarization states at the input and at the output stages. In the automated setup, all the optics are fixed so that there are no manual adjustments to the retardation and polarization of the beam of light. The automated system for obtaining the optical characteristics of a sample can be realized by using variable retarders and polarization rotators, which are voltage controlled.

The polarization rotators used in the set up are liquid crystal devices(MeadowLark Optics, CO), which consists of a retarder combined with a zero-order polymer quarter wave retarder. The fast axis of one retarder is oriented at 45 to the slow axis of the other. Polarization rotation is achieved by electrically controlling the retardance of the liquid crystal variable retarder, thus eliminating any mechanical motion.

The response time for the polarization rotator depends upon the desired rotation. Small rotations have longer response times. The voltages, required for a set of rotations of polarizers and retarders, are essential to obtain different orientations of the input and output polarization states. The polarization rotators are aligned such that the fast axis of the quarter wave retarder within the rotator is aligned in parallel to the transmission axis of the polarizers. The variable retarders used in the automated optical setup are also liquid crystal devices(MeadowLark Optics, CO), with the long axis of the liquid crystal molecules defining the extraordinary or slow index. The typical response time for the retarder is about 5ms to switch from one-half to zero waves and about 20ms to switch to switch from zero to one-half wave. The polarization rotators and the variable retarders are driven by an AC 2 kHz square wave of adjustable amplitudes with zero DC components for their optimum performance.

Thus, the different orientations of the input and the output polarization states can be obtained by controlling and changing the amplitudes of the AC square wave to the liquid crystal variable polarization rotators and the variable retarders.

Large collagen film(2×2 inches) was divided into four pieces and marked on the left corner of each piece to make sure all four pieces have the same fiber orientation. Three pieces were denatured in the temperature controlled water bath for three different heating times at 30 seconds, 2.5 minutes, and 6 minutes. Water temperature was maintained at 65 °C with the electric heater and controller. The temperature variance was ± 1 °C. Then denatured collagen samples were recovered in the room temperature water bath for 30 minutes. So one native and three differently denatured samples were prepared.

Each sample was sandwiched between microscope slides and mounted onto the sample rotator. The Mueller matrix measurements were performed by rotating the samples from 0 - 180 degrees to test the effect of fiber orientation and find out the rotation angle for the maximum differences between the native and three denatured samples.

In order to fully characterize the polarization state of the light passing through the sample, the 16 elements of the 4 4 Mueller Matrix was acquired via 36 images using various

input and output polarization optics. These 36 images consist of combinations of Horizontal(H), Vertical(V), + 45(P), - 45(M), Right circular(R), and Left circular(L) polarized light, at the input and output stage. The different combination of input and output polarization states that formulate an element in the Mueller matrix is represented in the equation 4.

The CCD camera allows us to image the varying intensities across the entire area, thus having an advantage over the single point silicon detector. The camera has an in-built software that permits the automatic opening of the shutter, clearing of the CCD array, collecting the images, averaging the images, removing the noise, and digitizing of the images.

B. Finding Fiber Orientation

The Mueller matrix results depend on the fiber orientation of the sample. Thus the information of the gross fiber orientation of the sample is required. Sacks et al. [27] showed that light is scattered perpendicular to the fiber axes and the light scattering pattern is symmetric about the preferred fiber direction(see Fig. 2). The fibrous network of the sample optically behaves like a two-dimensional assembly of single slits with assumption of no optical interactions. According to single-slit diffraction theory, light is scattered in a direction perpendicular to the fiber axis [28].

Fig. 3 shows the setup to find out the fiber orientation. A HeNe laser(633 nm) was used as light source and the collagen sample, which was sandwiched between microscope slides, was mounted on the rotator. The detector placed away from the optic center with distance R(the maximum scattering radius). The beam after passing through the sample showed the similar scattering pattern in Fig. 2. Thus, by rotating the sample, the peak intensity could be found with the detector and the optometer. Because light is scattered perpendicular to the fiber direction, the angular fiber orientation can be calculated as below.

$$\Phi = \theta_p + 90^\circ \tag{5}$$

where Φ is the angular fiber orientation and θ_p is the sample rotation angle at peak intensity.

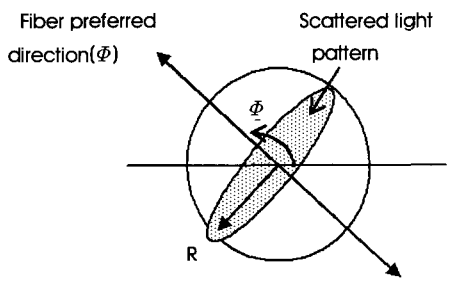

Fig. 2. The scattered light pattern due to fiber orientation.

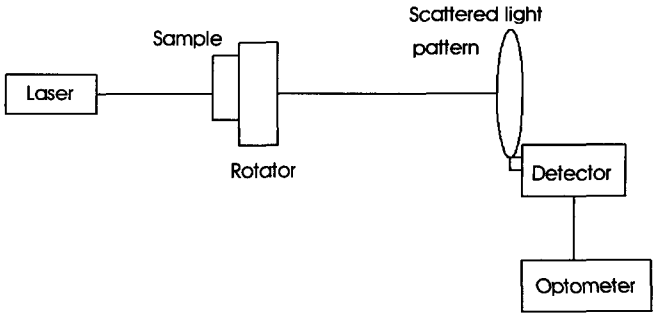

Fig. 3. The setup for finding the fiber orientation.

III. RESULTS AND DISCUSSION

A. Fiber Orientation

The scattered beam intensity was measured with the setup described in Fig. 3. The native collagen sample rotated with 10 degree increments over the 360 degree range. Near the angle of the peak intensity, the scattered beam intensity was detected with 2 degree increments.

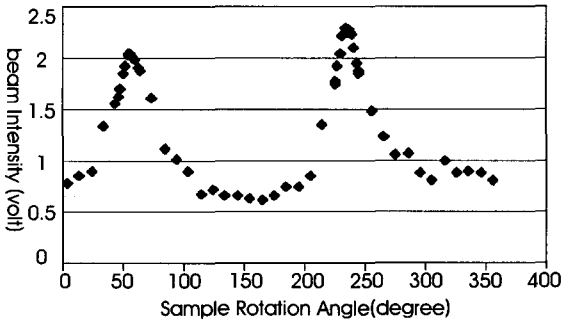

Fig. 4. Beam intensity changes due to sample rotation.

Two peaks were detected at the rotation angles of 54° and 234° over the 360° range. Thus, the fiber angular orientation can be represented by the equation 5. ($\Phi = \theta_p + 90^\circ = 54^\circ + 90^\circ = 144^\circ$) Fig. 4 shows the light scattering pattern is nearly symmetric about the preferred fiber direction. This measured fiber orientation was used as a standard for the Mueller matrix experiments.

B. Mueller Matrix Experiments

The Mueller matrix elements were obtained for each collagen sample using the automated system. These measurements were performed with rotating the sample at 0 , 45, 90, 135, and 180 and repeated three times. One native and three differently

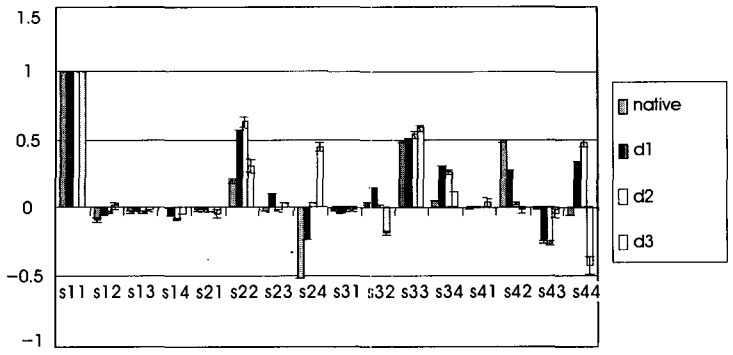

Fig. 5. The effect of the thermal damage of collagen sample on the Mueller matrix elements at the sample rotation angle $\theta = 0°$ (Native: No heat damage, d1: Tissue damage level 1, d2: Tissue damage level 2, d3: Tissue damage level 3).

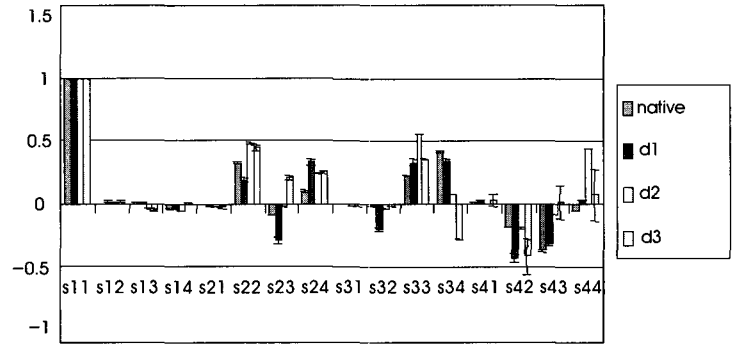

Fig. 6. The effect of the thermal damage of collagen sample on the Mueller matrix elements at the sample rotation angle $\theta = 45°$ (Native: No heat damage, d1: Tissue damage level 1, d2: Tissue damage level 2, d3: Tissue damage level 3).

denatured states were investigated in this study.

To determine each of the 16 Mueller matrix elements, a total of 36 images were taken at various combinations of input and output polarization states. Each of 16 experimental elements was calculated by adding or subtracting a series of image data according to equation 4. The individual Mueller matrix elements(s11, s12, s13, and etc.) are represented by a two-letter combination that denotes the input polarization and output analyzer orientation(i.e., s11= HH+HV+VH+VV, and HV denotes horizontal input polarization and vertical output polarization analyzer). The corresponding symbols denoting polarization are H(horizontal), V(vertical), P(+45°), M(-45°), R(right circular), and L(left circular). The Mueller matrix of the mirror was experimentally obtained and corrected for calculating the Mueller matrix of the collagen sample. The experimental setup shown in Fig.1 can be easily converted to measure the backscattering Mueller matrix of the actual animal skin in vivo by removing the mirror and put the animal at the mirror position.

Fig. 5 shows the effect of the thermal damage of collagen sample on the Mueller matrix elements at the sample rotation angle $\theta = 0°$. Because the fiber angular orientation is 144° with no rotation of the sample, the actual fiber orientation is also 144° in this position. The denatured samples which are denoted as d1, d2, and d3 were thermally treated in the 65°C water bath for 0.5, 2.5, and 6 minutes, respectively. The temperature of the water bath was controlled by the electric heater with ± 1°C variance.

Each of the individual elements has been normalized with respect to the s11 element of the Mueller matrix. Thus s11 is always 1 and the standard deviation of s11 is 0. The elements s12, s13, s14, s21, s31, and s41 show small values while the s22, s24, s33, s42, and s44 shows large values. The elements s12, s24, and s33 are increased with increasing thermal damage while s42 is decreased as thermal damage increases. The elements s22, s32, and s44 show up and down pattern for thermal damage changes.

The effect of thermal damage on the Mueller matrix at the sample rotation angle $\theta = 45°$ is shown in Fig. 6. The fiber angular orientation is 189° in this position. The elements s12, s13, s14, s21, s31, and s41 do not show any considerable change for different heating levels. The element s34 shows the

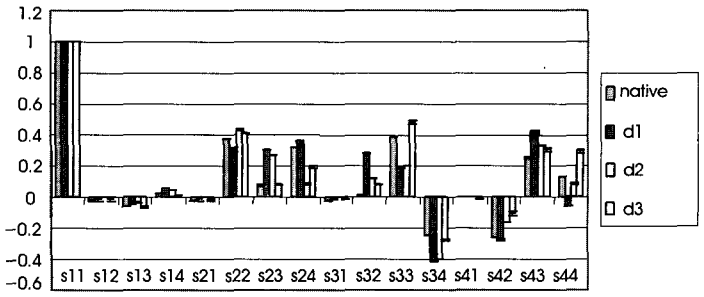

Fig. 7. The effect of the thermal damage of collagen sample on the Mueller matrix elements at the sample rotation angle = 90 (Native: No heat damage, d1: Tissue damage level 1, d2: Tissue damage level 2, d3: Tissue damage level 3).

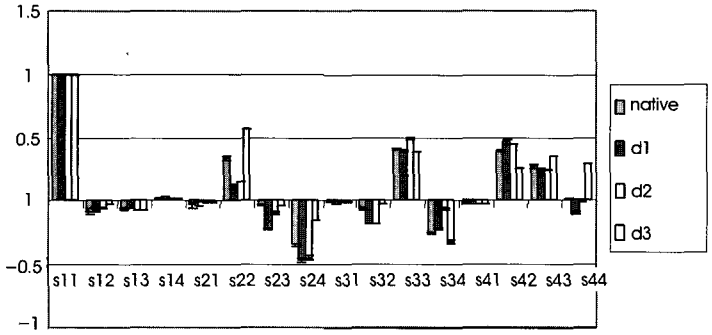

Fig. 8. The effect of the thermal damage of collagen sample on the Mueller matrix elements at the sample rotation angle = 135 (Native: No heat damage, d1: Tissue damage level 1, d2: Tissue damage level 2, d3: Tissue damage level 3).

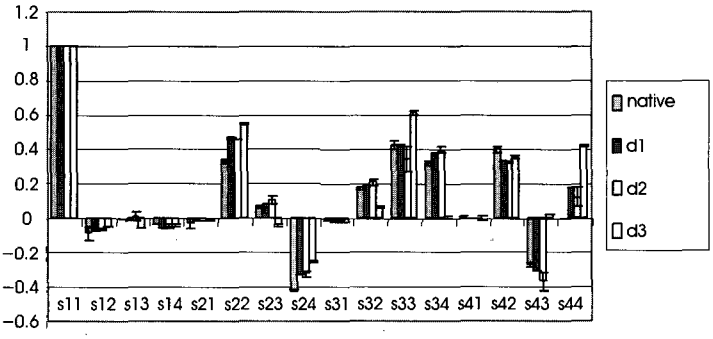

Fig. 9. The effect of the thermal damage of collagen sample on the Mueller matrix elements at the sample rotation angle = 180 (Native: No heat damage, d1: Tissue damage level 1, d2: Tissue damage level 2, d3: Tissue damage level 3).

decreasing trend with increasing thermal damage while s43 is increased as thermal damage increases. The other elements such as s22, s23, s24, s33, s42, and s44 show irregular changes.

Fig. 7 shows the effect of thermal damage on the Mueller matrix at the sample rotation angle $\theta = 90$. Thus the fiber orientation is 234 . The elements s12, s13, s14, s21, s31, and s41 show weak signals over the all heating levels including the native state. Only the element s42 shows increasing trend with increasing thermal damage. The other elements are showing no pattern even though they show considerable changes due to thermal damage.

At the sample rotation angle $\theta = 135$ (the finer orientation is 279), the thermal damage effect on the Mueller matrix is shown in Fig. 8. Similarly, the elements s12, s13, s14, s21, s31, and s41 show small values and the element s12 shows slightly increasing trend for the increased thermal levels. The elements s22, s23, s24, s32, s33, s34, s42, s43, and s44 show changes but no considerable pattern for thermal damage changes.

The effect of the thermal denaturation at the rotation angle $\theta = 180$, so the fiber orientation is 324 , is shown in Fig. 9. Again, the elements s12, s13, s14, s21, s31, and s41 show small values. The elements s22, s24, s33 show large values and increasing pattern with increasing thermal damage level while other elements show no trend.

The Fig. 10 shows the comparison between the changes of the Mueller matrix elements and the scattering changes. The scattering coefficients of the native and three denatured samples were determined with integrating sphere technique. Each change ratio was calculated with respect to the each value at the native state. The Mueller matrix elements at the sample rotation angle $\theta = 0$ were used for these calculations because the changes and trend at this orientation were the most considerable.

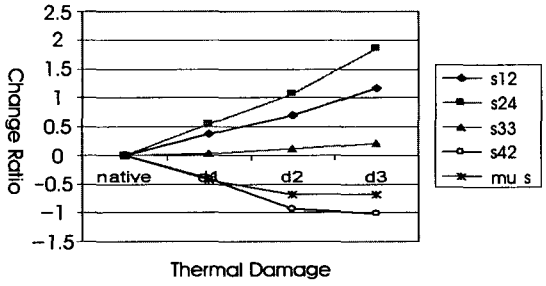

Fig. 10. Mueller element changes vs. scattering changes (Native: No heat damage, d1: Tissue damage level 1, d2: Tissue damage level 2, d3: Tissue damage level 3, mu_s : reduced scattering coeffiecent).

The Mueller matrix elements s12, s24, and s33 show increasing trend as thermal damage increases. The maximum change of the element s24 is + 186% at the highest heating level. The elements s12 and s33 show the changes of up to + 117% and + 20.8%, respectively. The element s42 shows decreasing trend in thermal denaturation and the maximum change is - 102%. The scattering coefficient decreases up to - 68% with increasing thermal damage. The scattering change is saturated at the second heating level (d2). However, the Mueller elements are not saturated in this heating range.

To investigate the effect of the fiber orientation on the Mueller matrix, each element was averaged over the all sample rotation angles. In general, large standard deviations in the native state which mean the effect of fiber direction on the Mueller matrix is considerable. With increasing thermal damage, the standard deviations of the Mueller matrix elements are decreasing. The results imply that the effect of fiber orientation on the Mueller matrix decreases as thermal damage increases.

Ⅳ. CONCLUSIONS

The Mueller matrix elements were obtained for native and denatured collagen samples at different sample rotation angles using the automated data acquisition system. The changes of the Mueller elements depended on the sample rotation angle or fiber orientation. These changes decreased as thermal damage increased because of the increased randomness of fiber formation due to thermal denaturation. This implies the birefringence loss of collagen due to thermal denaturation.

For a certain fiber orientation, some of the Mueller matrix elements such as s24 and s33 showed an increase with increasing thermal damage level while s42 showed the decreasing pattern. According to the comparison between the changes in the Mueller matrix elements and in scattering, the scattering changes saturated in the applied damage range while some of the Mueller elements continuously changed. The changes of polarization characteristic represented by the Mueller matrix can be used as a tool for determining the thermal damage extent of the collagen sample.

REFERENCES

[1] G.L. Coté, M.D. Fox, and R.B. Northrop, "Noninvasive optical polarimetric glucose sensing using a true phase technique," *IEEE Trans. Biomed. Eng.*, vol. 39, no.7, pp. 752-756, 1992.

[2] G.L. Coté, "Noninvasive optical glucose sensing: an overview," *J. Clinic. Eng.*, vol. 22, no.4, pp. 253-259, 1997.

[3] G.L. Coté and B.D. Cameron, "Noninvasive polarimetric measurement of glucose in cell culture media," *J. Biomed. Optics*, vol. 2, pp. 275-281, 1997.

[4] W.F. March, B. Rabinovitch, and R.L. Adams, "Noninvasive glucose monitoring of the aqueous humor of the eye: Part 1. Measurement of very small optical rotations," *Diabetes Care*, vol. 5, pp. 254-268, 1982.

[5] W.F. March, B. Rabinovitch, and R.L. Adams, "Noninvasive glucose monitoring of the aqueous humor of the eye: Part 2. Animal studies and the scleral lens," *Diabetes Care*, vol. 5, pp. 259-265, 1982.

[6] G.L. Coté, M.D. Fox, and R.B. Northrop, "Laser polarimetry for glucose sensing," *Annual International Conference IEEE-EMBS*, vol. 12, no.2, pp. 476-477, 1990.

[7] G.L. Coté, Development of a Robust Optical Glucose Sensor, Ph.D. Dissertation, University of Connecticut, Storrs, CT, 1992.

[8] G.L. Coté and B.D. Cameron, "Noninvasive polarimetric measurement of glucose in cell culture media," *J. of Biomed. Optics*, vol. 2, pp. 275-281, 1997.

[9] M. Goetz, *Microdegree Polarimetry for Glucose Detection*, M.S. Thesis, University of Connecticut, Storrs, CT, 1992.

[10] M. Goetz, M.D. Fox, and R.B. Northrop, "Microdegree polarimetry using a diode laser for glucose detection," *Annual International Conference IEEE-EMBS*, Paris, France, vol. 2, pp. 97-98, 1992.

[11] M. Michael, *Multispectral glucose sensing using a polarimetric differencing technique*, M.S. Thesis, Texas A&M University, College Station, TX, 1995.

[12] B.D. Cameron, *Polarimetric glucose sensing utilizing a digital closed loop system*, M.S. Thesis, Texas A&M University, College Station,TX, 1995.

[13] T.W. King, G.L. Coté, R. McNicols, and M.J. Goetz, "Multispectral polarimetric glucose detection using a single pockels cell," *Opt. Eng.*, vol. 33, pp. 2746-2753, 1994.

[14] B.D. Cameron and G.L. Coté, "Non invasive glucose sensing utilizing a digital closed-loop polarimetric approach," *IEEE Trans. Biomed. Eng.*, vol.44, pp. 1221-1227, 1997.

[15] W.S. Bickel and W.M. Baily, "Stokes vector, Mueller matices, and polarized scattered light," *Optics Express*, vol. 1, pp. 441-454, 1997.

[16] W.S. Bickel, J.F. davison, D.R. Huffman, and R. Kilkson, "Application of polarization effects in light sacttering: a new biophysicical tool," in *Proc. Natl. Acad. Sci.* USA, 1976, vol. 73, pp. 486-490.

[17] A.H. Hielscher, J.R. Mourant, and I.J. Bigio, "Influence of particle size and concentration on the diffuse backscattering of polarized light from tissue phantoms and biological cell suspensions," *Applied optics*, vol. 36, pp. 125-135, 1997.

[18] A.H. Hielscher, A.A. Eick, J.R. Mourant, and D. Shen, J.P. Freyer, and I.J. Bigio, "Diffuse backscattering Mueller matrices of highly scattering media," *Optics Express*, vol.1, pp. 441-454, 1997.

[19] B. V. Bronk, W.P. van De Merwe, and M. Stanley, "An in vivo measure of average bacterial cell size from polized light scattering-function," *Cytometry*, vol. 13, pp. 155-162, 1992.

[20] W.P. van De Merwe, D.R. Huffman, and B.V. Bronk, "Reproducibility and sensitivity of polarized light scattering for identifying bacterial suspensions," *Applied Optics*, vol. 28, pp. 5052-5057.

[21] S. Zeitz, A. Belmont, and C. Nicolini, "Differential scattering of circularly polarized light as a unique probe of polynucleosome superstructure," Cell. Biophys., vol. 5, pp. 163-187, 1983.

[22] A.H. Hielscher, A.A. Eick, J.R. Mourant, J.P. Freyer, and I.J. Bigio, "Biomedical diagnostic with diffusly backscattered linearly and circularly polarized light," *SPIE Proc.*, vol. 2976, pp. 298-305, 1997.

[23] M.J. Racovic, G. kattawar, M Mehrubeoglu, B. D. Cameron, S. Rastegar, L.V. Wang, and G.L. Coté, "Light backscattering polarization patterns from tubid media: theory and experiment," *Applied Optics*, vol. 38, pp. 3399-3408,1999.

[24] A. Ambrirage and D.C. Look, "A backward Monte Carlo study of the multiple scattering of a polarized laser beam," *J. Quantum Spectrosc. Radiat. Transfer*, vol. 58, pp. 171-192, 1997.

[25] B. D. Cameron, M.J. Racovic, M Mehrubeoglu, G. kattawar, S. Rastegar, L.V. Wang, and G.L. Coté, "Measurenment and calculation of the two-dimensional backscattering Mueller matrix of a turbid medium," *Optics Letter*, vol.23, pp. 485-487, 1998.

[26] B. D. Cameron, M.J. Racovic, M Mehrubeoglu, G. kattawar, S. Rastegar, L.V. Wang, and G.L. Coté, "Measurenment and calculation of the two-dimensional backscattering Mueller matrix of a turbid medium: errata," *Optics Letter*, vol.23, pp. 1630, erratum, 1998.

[27] M.S. Sacks, D.B. Smith, and E.D. Hiester, "A small angle light scattering device for planar connective tissue microstructural analysis," *Annals Biomed. Eng.*, vol. 25, pp. 678-689, 1997.

[28] M.S. Sacks, C.J. Chuong, W.M. Petroll, M. Kwan, and C. Halberstatd, "Collagen fiber architecture of a cultured tissue," *J. Biomech. Eng.*, vol. 119, pp.124-127, 1997.